Global Ecology and Biogeography

WILEY

Global Ecology and Biogeography | A Journal of Macroecology

DATA ARTICLE OPEN ACCESS

CoralBleachRisk—Global Projections of Coral Bleaching Risk in the 21st Century

Camille Mellin[1,2] | Stuart Brown[1] | Scott F. Heron[3] | Damien A. Fordham[1]

[1]The Environment Institute and School of Biological Sciences, University of Adelaide, Adelaide, South Australia, Australia | [2]South Australian Research and Development Institute (Aquatic Sciences), West Beach, South Australia, Australia | [3]Physics and Marine Geophysical Laboratory, College of Science and Engineering, James Cook University, Townsville, Queensland, Australia

Correspondence: Camille Mellin (camille.mellin@adelaide.edu.au)

Received: 8 August 2024 | **Revised:** 10 December 2024 | **Accepted:** 3 January 2025

Handling Editor: Jonathan Belmaker

Funding: This work was supported by the Australian Research Council through grants FT200100870 (C.M.) and DP230102986 (S.F.H.); SUBAK (S.B.); the University of Adelaide Environment Institute.

Keywords: bleaching alert | climate change | coral reefs | degree heating weeks | future forecasts | global warming | marine heatwaves

ABSTRACT

Motivation: Timing, duration and severity of marine heatwaves are changing rapidly in response to anthropogenic climate change, thereby increasing the frequency of coral bleaching events. Mass coral bleaching events result from cumulative heat stress, which is commonly quantified through degree heating weeks (DHW). Here we introduce *CoralBleachRisk*, a daily-resolution global dataset that characterises sea surface temperatures, heat stress anomalies and the timing, duration and magnitude of severe coral bleaching conditions from the recent past (1985) to the future (2100) under three contrasting Shared Socioeconomic Pathways. Our projections are downscaled to a 0.5° resolution (~50 km), bias-corrected and validated using remotely sensed data of sea surface temperatures and a global dataset of historical coral bleaching events. An accompanying online software tool allows non-specialist users to access aggregated metrics of coral bleaching risk and generate time series projections of coral vulnerability for Earth's coral reefs. Our dataset enables regional to global comparisons of future trends in severe coral bleaching risk.

Main Types of Variables Contained: Sea surface temperature (SST), SST anomaly, DHW, annual timing and duration of Bleaching Alerts.

Spatial Location: Global.

Time Period: 1985–2100.

Major Taxa and Level of Measurement: Coral communities.

Software Format: Netcdf (.nc).

1 | Introduction

Among all marine ecosystems, coral reefs and the ecosystem services they deliver to nature and humanity are the most at risk of human-driven climate impacts (Hughes et al. 2017). This is because reef-building corals live close to their upper thermal tolerance thresholds (Heron, Maynard, et al. 2016), making them particularly susceptible to mean annual anthropogenic warming of Earth's oceans (Hoegh-Guldberg et al. 2018). However, an even more pervasive human-driven climate threat to coral reefs is the increasing frequency and severity of acute marine heatwaves, a modern phenomenon causing recurrent

mass coral bleaching events at regional scales (>1000km) (Hughes, Anderson, et al. 2018) and, in many cases, coral mortality. Globally, the annual risk of coral bleaching increased from 18% to 31% in the three decades leading up to 2016, along with a 4.6-fold reduction in the return time of severe bleaching events (Hughes, Anderson, et al. 2018). In some severe marine heatwave events, corals have died directly from rapid-onset extreme heat (Leggat et al. 2019).

Coral bleaching—paling of the coral host—occurs when symbiotic microalgae (zooxanthellae, i.e., *Symbiodinium* spp.) leave the coral tissue after prolonged heat stress, resulting in coral mortality if cumulative heat stress is prolonged (Brown 1997; Spalding and Brown 2015). Risk of coral bleaching and subsequent mortality is commonly predicted using a cumulative metric of heat stress called degree heating weeks (DHW)—the sum of all positive anomalies above a maximum monthly mean (MMM) sea surface temperature (SST) threshold over a 12-week rolling window (Eakin et al. 2010; Liu et al. 2014). Although there is a strong correlation between maximum annual DHW and the probability of severe coral bleaching (and also mortality), the strength of the relationship can vary spatially and temporally (Hughes et al. 2021), because of environmental filtering resulting from past severe bleaching events—this has been termed 'ecological memory' (Hughes, Kerry, et al. 2018).

A more rigorous understanding of the risk that 21st century climate change poses to coral bleaching is needed to inform present-day management of Earth's coral reefs and their ecosystems. Vital conservation strategies such as coral transplantation, genetic manipulation of corals and engineering coral ecosystems can only be implemented at relatively small spatial scales (Darling and Côté 2018; Ainsworth et al. 2020), with future risk of coral bleaching being an important determinant of their success. However, several methodological impediments have so far limited the ability to accurately pinpoint coral reef regions that are at lower risk of increased magnitude, duration and frequency of marine heatwaves. Firstly, most available projections of DHW derived from coupled Atmosphere–Ocean General Circulation Models (AOGCMs) have been compiled from monthly-averaged rather than daily SST data (e.g., van Hooidonk et al. 2015, 2016). This averaging masks important daily variation in temperature extremes, which accumulate as positive anomalies in the calculation of DHW (Liu et al. 2014). Secondly, most future projections of DHW are currently available at a near-native spatial resolution of AOGCMs (1°×1°) (Donner et al. 2005; van Hooidonk, Maynard, and Planes 2013; Logan et al. 2014; van Hooidonk et al. 2014; but see also van Hooidonk et al. 2015; van Hooidonk et al. 2016; Dixon et al. 2022). Thirdly, existing forecasts of DHW do not account for inter-model variability from multiple AOGCMs using multi-model ensemble averaging, which has been shown to achieve better projection performance, regionally and globally (Fordham, Wigley, and Brook 2011).

Here, we introduce *CoralBleachRisk*, a continuous gridded (0.5°×0.5° resolution) dataset of historic, current and future coral bleaching risk based on downscaled and bias-corrected daily projections of SST and DHW. Downscaled and bias-corrected daily estimates are provided between 1985 and 2100 under three different future emissions scenarios from eight CMIP6 coupled AOGCMs. Annual summary projections of severity, duration and onset of severe bleaching conditions are provided for three Shared Socioeconomic Pathways (SSP) for the period 1985 to 2100. Projections are available for individual AOGCMs and a multi-model average. Tests show that historical projections of climate and bleaching closely reconstruct observed SST and past bleaching events, providing good confidence in future projections. We present two forms of data validation: (i) a climatological validation against satellite SST observations and (ii) an ecological validation against a historical dataset of past coral bleaching events. Our global projections of future risk of coral bleaching provide conservation managers and policy makers with the data needed to quantify 21st century coral loss across the world's coral reef regions (Mellin et al. 2024).

2 | Methods

2.1 | Overview

An overview of the design of our dataset is provided in Figure 1. Briefly, daily simulated sea surface temperatures (SST) available from eight Atmosphere–Ocean General Circulation Models (AOGCMs) were retrieved from the open access Coupled Model Inter-comparison Project phase 6 (CMIP6) (Eyring et al. 2016) for the period 1985 to 2100 for three SSPs (O'Neill et al. 2017). Data were downscaled to a 0.5°×0.5° regular grid and bias-corrected against a high-resolution SST satellite dataset (Merchant et al. 2019). Downscaled and bias-corrected daily SST data were used to calculate: (i) SST anomalies exceeding a spatially resolved bleaching threshold (defined as the MMM SST—a commonly employed bleaching threshold [Eakin et al. 2010; Liu et al. 2014]); (ii) cumulative heat stress defined as degree heating weeks (DHW); and (iii) annual estimates of the onset, duration and severity of coral bleaching conditions with DHW ≥4°C-week or 8°C-week critical thresholds.

2.2 | Historical, Future and Observed Sea-Surface Temperature

2.2.1 | Shared Socioeconomic Pathways

The latest AOGCM simulations of future climate are based on a combination of SSP and forcing levels used by the Representative Concentration Pathways (RCP) in CMIP5 (van Vuuren et al. 2011). Three SSP scenarios were selected from hundreds of future climate scenarios currently available, to represent contrasting climate mitigation and adaptation challenges resulting in a wide range of different climatic futures (O'Neill et al. 2017; Riahi et al. 2017). These scenarios included 'Middle of the road', with medium socio-economic challenges for mitigation and adaptation (SSP 2–4.5); 'Regional rivalries', with high socio-economic challenges for mitigation and adaptation (SSP 3–7.0); and 'Fossil-fueled development', with high socio-economic challenges for mitigation and low socio-economic challenges for adaptation (SSP 5–8.5) (O'Neill et al. 2017). We chose these because they reflect the most plausible future scenarios (i.e., SSP2-4.5 and beyond [Pielke Jr, Burgess, and Ritchie 2022; Hoegh-Guldberg et al. 2023]). The SSP numerical designation for each simulation combines the socio-economic scenario and radiative forcing level reached at the end of the century; for example, SSP

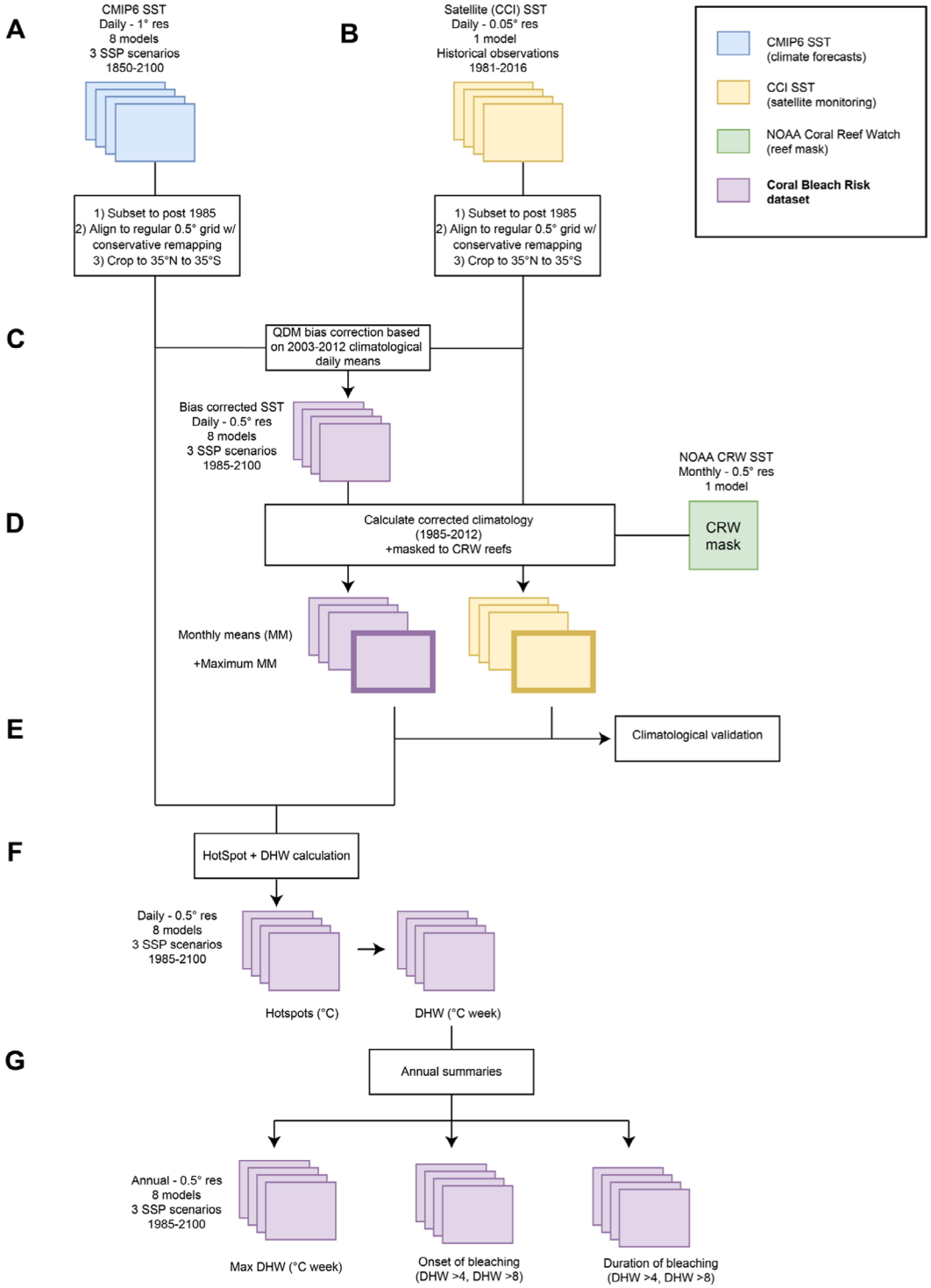

FIGURE 1 | Processing steps and design of the CoralBleachRisk dataset. (A) Simulated projections of sea surface temperatures (SST) from historical and future climates were extracted from eight CMIP6 climate models for the period 1985–2100. (B) Satellite observations of SSTs (1985–2016) were extracted from the CCI SST dataset. Datasets in A and B were re-gridded to a common 0.5°×0.5° resolution. (C) CMIP6 projections were bias-corrected against the CCI SST data using quantile delta mapping (QDM). (D) Climatological monthly mean SST were calculated from the downscaled and bias-corrected CMIP6 projections and CCI SST data. (E) CMIP6 projections of mean monthly SST were validated against CCI analysis data from 1985 to 2014. (F) Hotspots (°C) and degree heating weeks (DHW, °C-week) were calculated for each pixel at a daily resolution between 1985 and 2100. (G) Daily DHW data were used to calculate annual measures (onset, duration, severity) of severe bleaching risk in each pixel. These projections were validated against observations of coral bleaching for the period 1985–2010.

5–8.5 is a fossil-fuelled development scenario (SSP 5) with radiative forcing level reaching approximately 8.5 W/m^2 by 2100 (van Vuuren et al. 2011; Riahi et al. 2017).

2.2.2 | Historical and Future Climate Data

Historical and future climate datasets with daily simulated SST available for each of the three SSP were extracted from the open access CMIP6 Earth System Grid Federation data portal (https://aims2.llnl.gov/search, https://esgf-node.llnl.gov/search/cmip6/). Historical data (1850–2014) were accessed for eight CMIP6 AOGCMs that also had daily SST available for SSP scenarios 2–4.5, 3–7.0 and 5–8.5 (Eyring et al. 2016) (see Table 1 for model details). We used the historical climate simulations to test AOGCM performance against an observational dataset (see Section 2.7.1).

Future climate data were accessed for the period 2015–2100 for these same eight CMIP6 AOGCMs (Riahi et al. 2017). The SSP scenarios simulate possible future climates from 2015, having been initialized using the climate conditions at the end of the historical period in 2014 (Riahi et al. 2017). We used the first model realisation (r1i1p1f1) for each AOGCM, which is common practice in climate change assessment tools (e.g., MAGICC/SCENGEN [Fordham et al. 2012]). The rationale for this decision was that not all models had multiple realisations for the historical and future periods. Additionally, it has been established that projections of climate conditions improve with an increase in the number of ensemble-averaged models, not realisations (Pierce et al. 2009).

2.2.3 | Observational Data

Observed SST data were accessed from a high-resolution satellite-derived dataset (Merchant et al. 2019), which was created as part of the European Space Agency Sea Surface Temperature Climate Change Initiative (CCI) (Good et al. 2019) (hereafter CCI SST) available as an open access dataset at https://data.ceda.ac.uk/neodc/esacci/sst/data/CDR_v2/Analysis/L4/v2.1. This level-4 (L4) gridded CCI SST dataset is representative of global daily-mean SST (at 20 cm depth) from 1981 to 2016 on a 0.05° × 0.05° grid, with gaps between available daily observations filled statistically. Validation of the L4 product using in situ measurements of SST from drifting buoys shows excellent spatiotemporal agreement, particularly after 2003 (Merchant et al. 2019). A thorough product validation is provided in Rayner et al. (2019).

2.3 | Pre-Processing of Climate Data

Simulated and observed climate data are typically available over different temporal extents and spatial resolutions, which required several pre-processing steps to ensure that the datasets were harmonised consistently, and that all data were on a spatially consistent grid (Figure 1). All pre-processing was done using the Climate Data Operators (CDO) software (Schulzweida 2021) and netCDF Operators (NCO) software (Zender, Butowsky, and Vincente 2021).

2.3.1 | Re-Gridding

To enable spatially consistent comparisons across all input datasets, the CMIP6 projections and the CCI SST were re-gridded to a common 0.5° × 0.5° regular grid using conservative interpolation, an approach accounting for all source cells intersecting the destination cell and returning a weighted average (Jones 1999). Conservative interpolation was thus chosen to maintain areal averages between (i) the coarse CMIP6 grids, which themselves were on different grid scales (Table 1), and (ii) the finer scale analysis grid (Jones 1999).

TABLE 1 | Description of the eight AOGCMs used in our study. All Atmosphere–Ocean General Circulation Models (AOGCMs) had daily data available for the historical period (1850–2014) and three SSP scenarios (SSP2-4.5, SSP3-7.0, SSP5-8.5; 2015–2100). All models had a native nominal resolution of 1° × 1° and were re-gridded from their native non-regular grids to a regular 0.5° × 0.5° grid spanning 35° S to 35° N using conservative remapping. ECS = equilibrium climate sensitivity; change in global-mean air temperature due to an instantaneous doubling of CO_2. TCR = transient climate response; warming from a simulation that is driven by an exponential 1.0% per year increase in CO_2. Models with a TCR inside the 1.4°C–2.2°C range (indicated with an asterisk) are those included in the 5-model ensemble (*ens5*) as recommended (Hausfather et al. 2022).

Model	Institution(s)	Ocean model	ECS	TCR
BCC-CSM2-MR	Beijing Climate Center	MOM4-L40v2	3.02	1.59*
CanESM5	Canadian Centre for Climate Modelling and Analysis	NEMO-v3.4.1	5.64	2.66
CESM2	National Center for Atmospheric Research	POP2	5.15	2.04*
EC-Earth3	EC-Earth consortium	NEMO-v3.6	4.26	2.38
IPSL-CM6A-LR	L'Institut Pierre-Simon Laplace	NEMO-v3.6	4.70	2.32
MIROC6	Center for Climate System Research, the University of Tokyo, the Japan Agency for Marine-Earth Science and Technology, the National Institute for Environmental Studies	COCO-v4.5	2.60	1.52*
MRI-ESM2-0	Meteorological Research Institute	MRI.COM-v4	3.13	1.56*
NorESM2-MM	Norwegian Climate Consortium	BLOM	2.49	1.33*

This processing step was implemented with the *ncremap* function for NCO (Zender, Butowsky, and Vincente 2021). All regridded data were then cropped to latitudes between 35° N and 35° S where known coral reefs occur.

2.3.2 | Temporal Window

CMIP6 historical simulations start in 1850; however, only years since 1985 were included in *CoralBleachRisk* because of modern observations of occurrence of mass bleaching events only being available from this year. For all datasets, any leap days (29th February) were excluded from analysis as not all models contained leap days. To provide continuous estimates of SST between the historical and future periods, we harmonised the historic and forecast projections for each of the models by temporally merging past and future simulations (Santer et al. 2013; Brown et al. 2020).

2.4 | Bias Correction

Model bias correction is done to correct distributional biases in simulated climate data relative to historical climate observations (Fordham et al. 2017). We compared two-bias correction methods for our SST data: (i) a simple, commonly used delta change factor (CF) method and (ii) the quantile delta mapping (QDM) method, which is particularly suited to bias correcting climate data characterised by extremes and anomalies (e.g., rainfall and heatwaves) (Cannon, Sobie, and Murdock 2015).

The CF method calculates anomalies between climatological averages (i.e., a baseline climate) of observed and simulated climatic conditions, and then adds those anomalies to the simulated climate. QDM is a multi-step bias correction method consisting of: (i) detrending the individual quantiles; (ii) applying a regular quantile mapping to the detrended series; and (iii) re-applying the projected trends to the bias-adjusted quantiles (Cannon, Sobie, and Murdock 2015). Regular quantile mapping involves mapping n quantiles of the cumulative distribution function of all values from the baseline period of the simulated climate onto the quantiles of the cumulative distribution function of all values from the baseline of the observed climate.

For both methods, the baseline period of 2003–2012 was selected. This period was chosen because of the high quality of satellite data in the CCI SST analysis (Merchant et al. 2019; Rayner et al. 2019) and potential limitations in satellite-based detection of extreme temperature events before 2003 (Little et al. 2022). The model bias-corrected SST values from each method were then compared against the observational data (CCI SST) for the historical period (1985–2014) (see Section 2.7.1).

2.5 | Climate Indices of Coral Bleaching Risk

We calculated six climate indices of coral bleaching risk for each reef location identified from the NOAA Coral Reef Watch (CRW) dataset (Heron, Johnston, et al. 2016) (Figure 1). These heat stress metrics were as follows: (i) degree heating weeks (DHW, °C-week)—a cumulative metric of heat stress; (ii) annual maximum DHW; (iii) the 99th percentile of DHW in each year; (iv) the annual number of days at or above DHW thresholds of 4°C-week and 8°C-week (Liu et al. 2014). To calculate timing of onset of severe bleaching, we also calculated: (v) the day of year when DHW first exceeds 4°C-week and 8°C-week thresholds; and (vi) the day of year when DHW exceeds 4°C-week and 8°C-week, relative to the climatological coldest day of year in each coral reef pixel. The latter allowed global comparisons of the onset of bleaching conditions despite differences in the seasonality of SST between hemispheres. The calculation of each metric is detailed below.

2.5.1 | Maximum Monthly Mean

The calculation of DHW requires defining the maximum monthly mean SST in each grid cell. The original CRW climatology was created by averaging SST data from 1985 to 1990 and 1993 (at that time, the 1991–1992 data were unreliable because of the eruption of Mt. Pinatubo; Heron et al. 2014). This sets the corresponding time point for the historical baseline temperature to be in the early part of the year 1988. Here, following the current CRW methodology, daily (bias-corrected) SST data at each pixel were averaged for each individual month through the 28-year period 1985–2012 to produce 336 (28×12) monthly mean SST values. Averaging values for each calendar month (i.e., each January, then each February, etc.) across the 28-year period would result in a substantial modification to the historical time point (to the middle of 1998) and, in an era of warming, baseline temperature in reef locations. To account for the climate drift in observed and modelled SST, we used linear regressions of monthly mean SST values to set the 28-year climatological monthly mean SST for each reef pixel to the original historical time point (Heron et al. 2015). This technique was implemented to combine the benefit of a 'long' climatology period whilst acknowledging that warming has occurred in reef locations (Heron et al. 2015). From these location-specific, time-adjusted monthly mean climatology values, the maximum monthly mean (MMM) was determined as the maximum among the 12 monthly mean climatology values for each pixel.

2.5.2 | HotSpot Metric and Degree Heating Weeks

Daily SST anomalies (i.e., HotSpots [Liu et al. 2014]) for day i (HS_i, in °C) were calculated as the difference between SST_i and MMM. DHW_i (°C week) was then calculated as the cumulative sum of HotSpots above the MMM for each pixel over a rolling 12-week (84 day) window ending on day i as:

$$HS_i = \begin{cases} SST_i - MMM, & \text{if } SST_i > MMM \\ 0, & \text{if } SST_i \le MMM \end{cases}$$

$$DHW_i = \sum_{n=i-83}^{i} \left(\frac{HS_i}{7} \right), \quad \text{where } HS_i > 0$$

Traditionally, DHW values have been calculated using HotSpots of 1°C or greater as a high-pass filter (Liu et al. 2014; Skirving et al. 2020). However, recent work has shown an increase in the ability of statistical models to predict coral bleaching events using accumulations of all $HS_i > 0$°C as in this study (Lachs et al. 2021).

2.5.3 | Magnitude, Duration and Onset of Bleaching Conditions

In each year from 1985 to 2100, we calculated the magnitude of coral bleaching risk as the annual maximum DHW in each pixel.

We calculated the duration of coral bleaching conditions to capture observations that exposure to summer-like temperature conditions is becoming longer, and the period of winter reprieve from warm temperatures is decreasing (Heron, Maynard, et al. 2016). The duration of coral bleaching conditions was defined as the total number of days, in a given year, when DHW exceeds the critical thresholds of 4°C-week and 8°C-week. These thresholds have been associated with significant coral bleaching (i.e., Bleaching Alert Level 1) and widespread bleaching and coral mortality (i.e., Bleaching Alert Level 2), respectively (Liu et al. 2014), and remain applicable when accumulating all $HS_i > 0$°C (Lachs et al. 2021) (including within the bleaching outlook prediction tool [Liu et al. 2018]).

We defined the onset of bleaching and severe bleaching conditions by the day number of each calendar year when DHW exceeds 4°C-week and 8°C-week, respectively. To allow global comparisons of the onset of bleaching conditions that account for differences in seasonality between hemispheres, we also calculated relative onset of bleaching as the number of days since 'mid-winter' when DHW first exceeds 4°C-week and 8°C-week. Here, mid-winter was defined as the climatological coldest day of the year for each pixel from the bias-corrected SST over the baseline period of 2003–2012.

2.6 | Multi-Model Ensemble

We generated a five-model ensemble average (hereafter '*ens5*') based on five CMIP6 models that had a transient climate response (TCR; i.e., warming from a simulation that is driven by an exponential 1.0% per year increase in CO_2) inside the 1.4°C–2.2°C range as recommended by Hausfather et al. (2022) (Table 1). Previous research using CMIP5 simulations has shown that the skill of multi-model ensemble averages to reproduce observed climate patterns asymptotes when at least five different models have been averaged (Pierce et al. 2009).

2.7 | Validation

2.7.1 | Statistical Validation

A two-stage statistical validation was done to (i) identify the best bias-correction method (i.e., CF or QDM) based on model agreement with the CCI SST data at a regional scale, and (ii) for the best bias-correction method (i.e., QDM—see Section 3), calculate the agreement between these modelled bias-corrected estimates and the CCI SST data at a global scale. For (i), we chose the north-eastern Australian region (140° E–160° E, 30° S–10° S) because CCI analysis SST data has been shown to be highly consistent with in situ local-scale measurements of SST at shallow reefs (Rayner et al. 2019); and because processing constraints prevent doing these tests over larger geographic extents.

We used the Kling-Gupta efficiency (KGE) metric (Gupta et al. 2009) that ranges from −Infinity to 1, with values closer to 1 indicating more agreement between the bias-corrected and CCI SST data. Each model's daily and monthly climatological means, and those of *ens5*, were compared with the corresponding CCI SST values over the 1985–2014 period. The comparison was done using Taylor diagrams that display correlations and standard deviations between the bias-corrected and observed data.

We also calculated multiple statistical metrics to quantify the relationship between our QDM bias-corrected SST estimates and the CCI SST data for each of the 25 AR6 Working Group I reference regions (Iturbide et al. 2020) and the 40 Marine Ecoregions of the World (MEOW) (Spalding et al. 2007) provinces. These metrics were as follows: percentage bend correlation (Wilcox 1994), root mean square error, ratio of standard deviations and modified index of agreement (Willmott 2013). These metrics were first calculated using all cells within each of the IPCC AR6 reference and MEOW provinces and then using only cells containing coral reefs according to the NOAA Coral Reef Watch dataset (Heron, Johnston, et al. 2016) to ensure that the correlation between our bias-corrected estimates and the CCI SST data remained high when considering reef cells only.

2.7.2 | Ecological Validation

We tested the ability of our derived DHW metrics to predict the occurrence of past coral bleaching events (Donner, Rickbeil, and Heron 2017) within the IPCC AR6 regions. For this ecological validation, we used the open access global dataset of mass coral bleaching events collated by Donner, Rickbeil, and Heron (2017) that spans most of the historical baseline period (1985–2012). This was the most comprehensive dataset available at the time of project development and analysis (available at https://figshare.com/projects/Coral_Bleaching_Database_V1/19753). Here we only considered records of severe bleaching events (i.e., severity level 3). This is because reports of lower or unknown bleaching severity can potentially conceal greater bleaching impacts if surveys occurred before or after the peak of bleaching—an important source of uncertainty in voluntary and citizen science programmes (Suggett and Smith 2011; Donner, Rickbeil, and Heron 2017). This subset of the global mass coral bleaching dataset contained 1975 severe coral bleaching events that overlapped with our historical projections of maximum annual DHW based on both the CMIP6 models and with the CCI SST.

We quantified both the ability of DHW estimates from CMIP6 models and those calculated using CCI SST data to predict the

occurrence of observed severe bleaching events by calculating the hit rate (correctly projecting bleaching) (Spillman and Smith 2021) based on the global mass coral bleaching dataset. According to this method, if a model predicted a coral bleaching alert (DHW ≥ 4°C-week) within 18 months of an observed bleaching event, this event was termed a 'hit'. Alternatively, if no bleaching alert was predicted by the model (DHW < 4°C-week) within 18 months of an observed bleaching event, this event was termed a 'miss'. These 'hit' and 'miss' occurrences were combined within the hit rate as follows:

$$\text{Hit rate}_{(x,y,lt)} = \frac{\sum_t \text{Hit}_{(t,x,y,lt)}}{\sum_t \text{Hit}_{(t,x,y,lt)} + \sum_t \text{Miss}_{(t,x,y,lt)}},$$

where (x, y) is the pixel containing at least one coral bleaching event, t is the survey date, and lt is the lead time for predicted bleaching alerts (18 months). The use of hit rate removes any skill bias by incorporating only correct positives (i.e., where a bleaching prediction matched an observed bleaching event [Spillman and Smith 2021]). We then calculated and mapped the mean hit rate and its standard error for each individual model, the five-model ensemble average *ens5* and the CCI SST within each IPCC AR6 region.

We used beta-regression (Ferrari and Cribari-Neto 2004) to assess whether the proportion of severe bleaching events was well predicted by the *ens5* hindcast as well as the CCI SST. Here, we compared two global models with DHW values from either (i) the ens5 hindcast or (ii) CCI SST as the response variable, and the number of individual bleaching events in each IPCC region as the predictor. We first ran these models at a global scale and repeated them for each IPCC region. To ensure sufficient sample sizes, the validation analysis excluded seven (out of a total of 25 regions) IPCC regions that had < 10 severe bleaching records. The analysis was done using the rstanarm package in R (Goodrich et al. 2023). Models were constructed with normal priors ($\beta_k \sim \text{Normal}(0, 2.5)$) and four chains, each with 2000 samples, with the first 1000 samples being discarded as a burn-in. We ensured model convergence using Gelman–Rubin statistics (where values ≤ 1.1 were considered acceptable), along with testing for effective sample size, and visually examining trace-plots. We did posterior predictive checks to evaluate the model predictive accuracy relative to the observed data. We also plotted and compared the distribution of DHW values during severe bleaching events with that for all times within 1985–2012 at the same locations (i.e., baseline period) for both the *ens5* hindcast and the CCI analysis.

All analyses were performed in Climate Data Operators (CDO) software (Schulzweida 2021) and netCDF Operators (NCO) software (Zender, Butowsky, and Vincente 2021) and R version 4.4.4 (R Development Core Team 2022) using packages terra 1.6–48 (Hijmans 2022), sf 1.0–9 (Pebesma 2018), loader (Rodriguez, Jimenez, and Quiros 2024), rnaturalearth (South 2017), plotrix (Lemon 2006) and the climate4R package bundle (Iturbide et al. 2019).

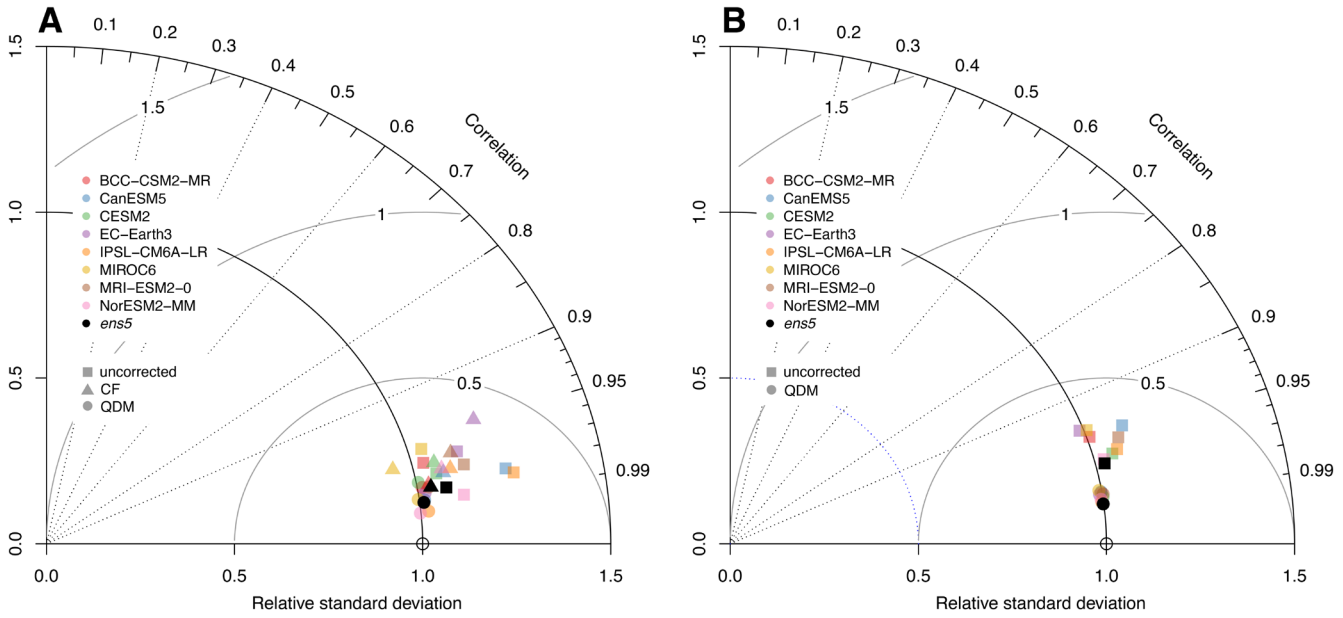

FIGURE 2 | Taylor diagrams comparing projected and observed mean monthly SST. Comparison of mean monthly SST from eight CMIP6 climate models with satellite (CCI SST data) over the period 1985–2014 for (A) Australia's Great Barrier Reef and (B) global coral reef regions. Uncorrected historical projections are shown as squares, change factor (CF) bias-corrected projections as triangles, and quantile delta mapping (QDM) bias-corrected projections as circles. Five-model ensembles (*ens5*) are shown for each of the datasets by the black dots. In both panels, colours represent different climate models (see inset key). A perfect model is one that corresponds to the empty black circle, that is, with the same standard deviation as the CCI SST data (i.e., relative standard deviation = 1), and a Pearson correlation coefficient of 1. Models closer to the origin are less variable than the CCI SST data (i.e., relative standard deviation < 1), those farther from the origin are more variable (i.e., relative standard deviation > 1). Models with an angle close to 0° from the *x*-axis are highly correlated to the CCI SST data (correlation ≈ 1), those with an angle close to 90° are little correlated (correlation ≈ 0).

3 | Results

3.1 | Statistical Validation

The QDM bias-correction method outperformed the simpler delta change factor (CF) method on Australia's Great Barrier Reef, which is the largest coral reef region in the world (Figure 2A). The strength of correlations with the satellite-derived observed SST (i.e., CCI SST) using monthly areal averages for both bias-correction methods was comparable (QDM = 0.99 ± 0.003; CF = 0.97 ± 0.005), whereas the ratio of standard deviations was improved for the QDM method relative to the CF method, indicating less inter-model spread in variability (QDM = 1.01 ± 0.01, CF = 1.04 ± 0.05) (Figure 2A). Significant improvements were shown for QDM over CF corrected datasets in the Kling–Gupta efficiency (KGE) metric comparing individual model daily average SST with the CCI SST (QDM = 0.91 ± 0.02, CF = 0.81 ± 0.07; $t(7) = 3.725$, $p = 0.007$). At a global scale, our results demonstrate excellent agreement between monthly QDM bias-corrected CMIP6 SST data and the CCI SST for the climatology period 1985–2014 (clustered circles in Figure 2B). Our five-model ensemble (*ens5*) hindcast was more skillful in capturing the observed SST conditions than any of the constituent models (Figure 2B).

Statistical validation of monthly climatological means for IPCC AR6 reference regions showed similar patterns (Figure 3), with average monthly percentage bend correlations of 0.91 (SD = 0.10). The *ens5* hindcast did better than the constituent models with an average monthly percentage bend correlation of 0.93 (SD = 0.07). Restricting the comparison to reef cells only decreased the average correlation across models and regions slightly to 0.86 (SD = 0.13), whereas for the *ens5* hindcast it reduced the bend

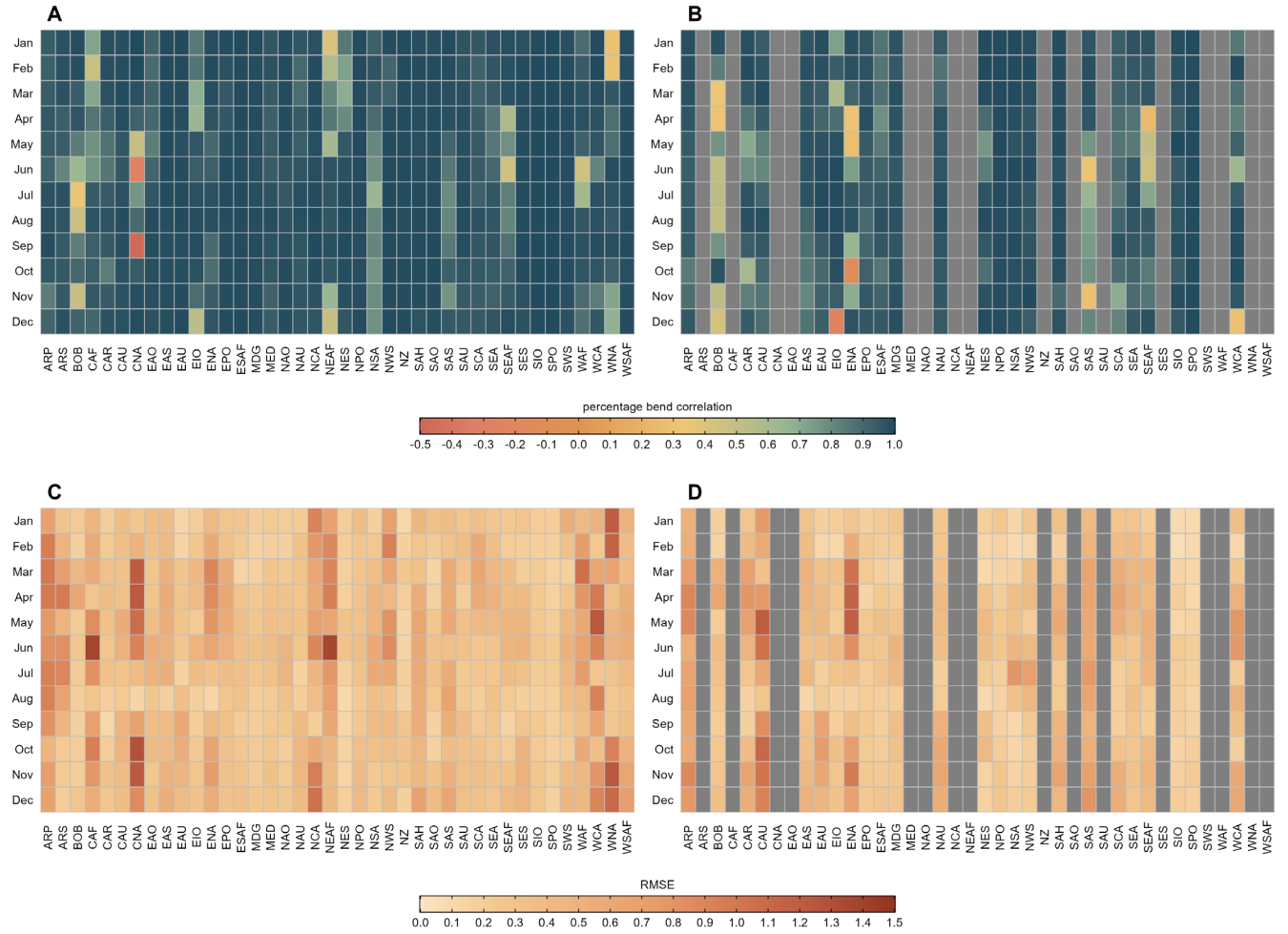

FIGURE 3 | Validation of SST values in IPCC AR6 reference regions. Comparison of QDM bias-corrected CMIP6 projections of monthly SST with CCI SST data for IPCC AR6 reference regions for the period 1985–2014. Results are shown for a five-model ensemble (*ens5*) projection. Upper panels show the percentage bend correlation (A) for all pixels and (B) reef cells only. Lower panels show the root mean square error (RMSE) for (C) all pixels and (D) reef cells only. Grey colour in (B) and (D) indicates no reef cells present in that specific region. With ARP: Arabian Peninsula; ARS: Arabian Sea; BOB: Bay of Bengal; CAF: Central Africa; CAR: Caribbean; CAU: C Australia; CNA: C North America; EAO: Equatorial Atlantic Ocean; EAS: E Asia; EAU: E Australia; EIO: Equatorial Indian Ocean; ENA: E North America; EPO: Equatorial Pacific Ocean; ESAF: E Southern Africa; MDG: Madagascar; MED: Mediterranean; NAO: N Atlantic Ocean; NAU: N Australia; NCA: N Central America; NEAF: N Eastern Africa; NES: NE South America; NPO: N Pacific Ocean; NSA: N South America; N W South America; NZ: New Zealand; SAH: Sahara; SAO: S Atlantic Ocean; SAS: S Asia; SAU: S Australia; SCA: S Central America; SEA: S E Asia; SEAF: S Eastern Africa; SES: S E South America; SIO: S Indian Ocean; SPO: S Pacific Ocean; SWS: S W South America; WAF: Western Africa; WCA: W C Asia; WNA: W North America; WSAF: W Southern Africa.

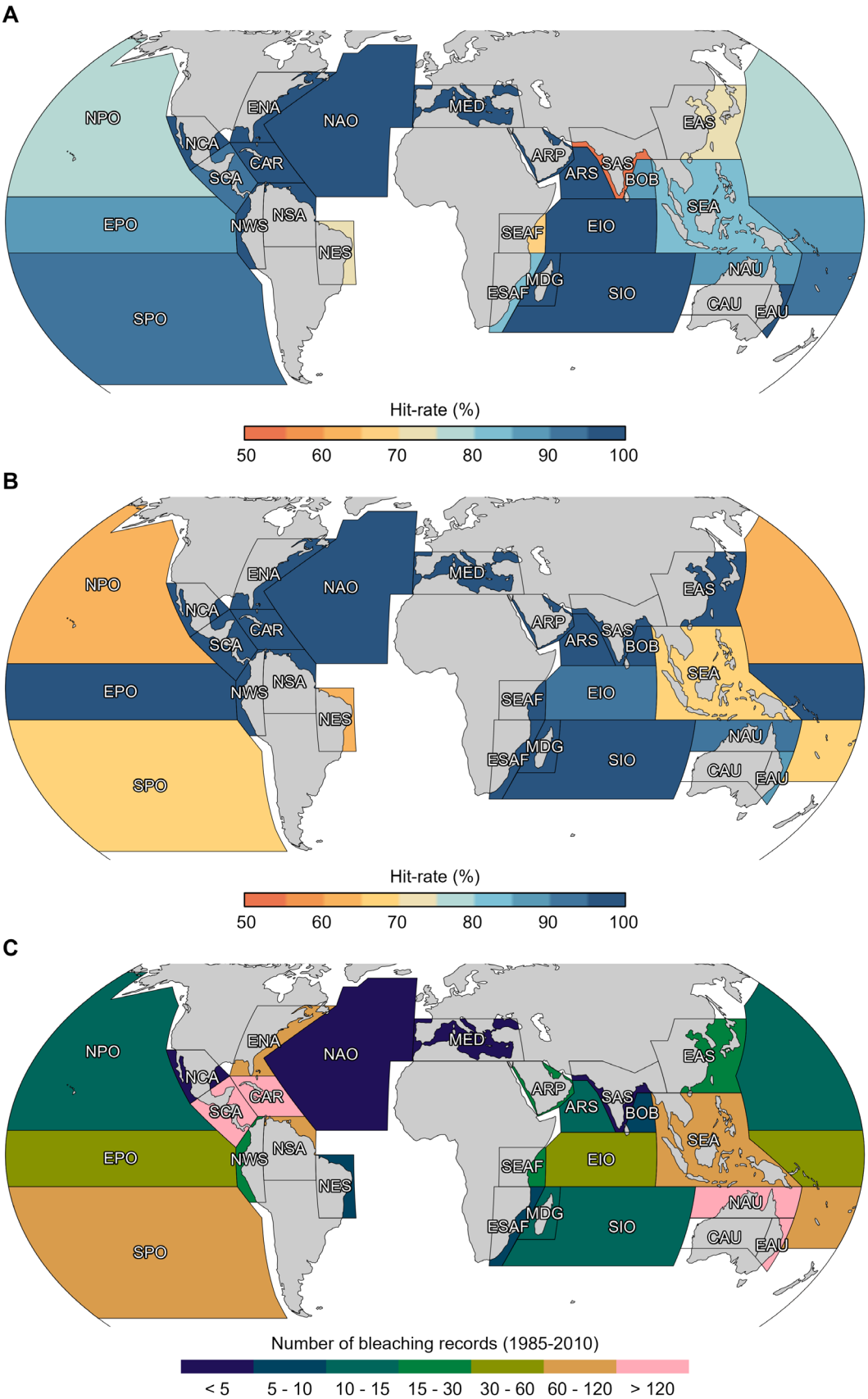

FIGURE 4 | Comparison of projected and observed bleaching events in IPCC AR6 regions. Percentage of successful bleaching events predicted (hit rate) between 1985 and 2012 for (A) the five-model ensemble (*ens5*) and (B) the CCI SST data. (C) The number of severe bleaching events (total = 1975) recorded in each IPCC AR6 region. Details of IPCC AR6 region codes are given in the Figure 3 caption.

correlation to 0.89 (SD = 0.09). Similar patterns were observed for RMSE with average values of 0.50 (SD = 0.23), and an *ens5* average of 0.42 (SD = 0.17) across all cells. RMSE values decreased when looking at reef cells only, with average values of 0.44 (SD = 0.19), and an *ens5* average of 0.38 (SD = 0.17). KGE statistics were between 0.51 and 0.77 depending on the model considered (mean = 0.68, SD = 0.08). The strength of the KGE statistic improved when using *ens5* (KGE = 0.81). The range of KGE statistic for all AOGCMs narrowed when using projections of SST for reef cells only, with values between 0.57 and 0.77; and the mean was marginally lower (mean = 0.66, SD = 0.09). Likewise, the KGE statistic decreased for the *ens5* hindcast for reef cells only (KGE = 0.73) compared with when including all cells.

Similar patterns were seen in the Marine Ecoregions of the World (MEOW) provinces, with an all-model-average monthly correlation of 0.86 (SD = 0.14) for the 163 MEOW provinces in our latitudinal range. This correlation increased for the *ens5* hindcast to 0.89 (SD = 0.10). RMSE values followed similar patterns with mean RMSE across all models of 0.43 (SD = 0.25) compared with 0.35 for *ens5* (SD = 0.18). Masking to reef cells decreased the average correlation to 0.81 (SD = 0.15) and 0.83 (SD = 0.13) for all models and the *ens5* hindcast, respectively. RMSE values improved when considering reef cells only, with average values of 0.35 (SD = 0.16) and 0.29 (SD = 0.12), respectively.

3.2 | Ecological Validation

Tests of projections of bleaching events against an existing dataset of coral bleaching (Donner, Rickbeil, and Heron 2017) show that both the *ens5* hindcast and the CCI SST predict bleaching events with high accuracy, with hit rates > 80% in 22 and 21 regions out of a total of 26 regions, respectively (Figure 4).

The region-level analysis indicated that *ens5* hindcast was better able to recreate the number of individual bleaching events than the CCI SST data in five of the 18 regions that had > 10 bleaching events recorded (Caribbean $\chi^2(1) = 5.88$, $p = 0.015$; South East Asia $\chi^2(1) = 3.89$, $p = 0.048$; Southern Pacific Ocean $\chi^2(1) = 18.58$, $p < 0.001$; Eastern Australia $\chi^2(1) = 11.43$, $p < 0.001$; South East Africa $\chi^2(1) = 4.16$, $p < 0.04$) (Figure 4). However, when comparing across all regions (i.e., globally), there was no statistical support that the *ens5* hindcast could more, or less, accurately predict the total number of regional scale bleaching events when

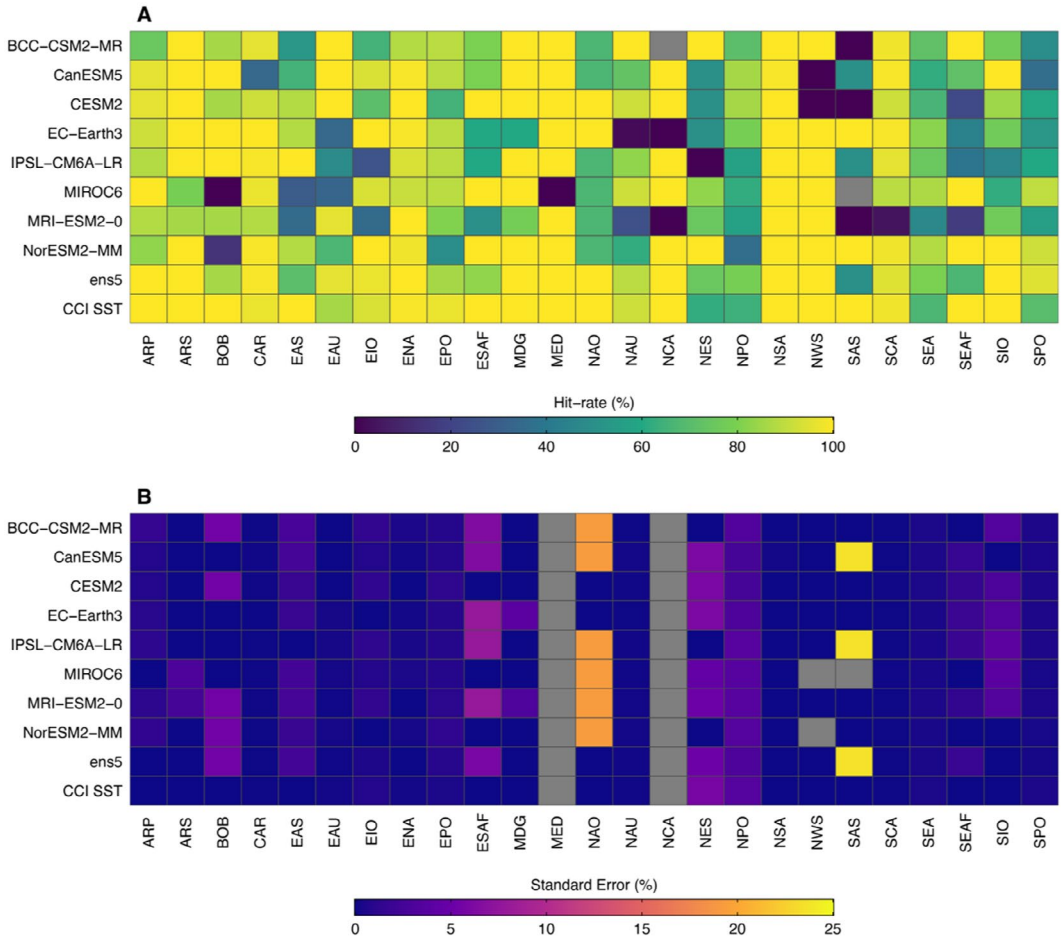

FIGURE 5 | Comparison of projected and observed bleaching events for individual climate models. Assessment of the ability of the downscaled and bias-corrected CMIP6 models to effectively predict observed coral bleaching events in IPCC AR6 regions measured as (A) mean % hit rate and (B) % hit rate standard error (SE). Grey colour for a given model × region combination indicates no data due to insufficient bleaching records. CMIP6 models (individual models and five-model average *ens5*) and the CCI SST are shown as rows, with IPCC AR6 regions shown as columns (see Figure 3 for a description of region names and Figure 4 for region locations).

compared to the CCI SST data ($V = 56$, $p = 0.552$). We found a mean hit rate of 90% (SD = 13%) across the IPCC AR6 regions the for *ens5* hindcast (Figure 4A), compared to a mean hit rate of 92% (S.D = 13%) from CCI SST data (Figure 4B). All posterior model checks, including the Gelman–Rubin statistic, effective sample size, and trace-plots, indicated that the models were constructed correctly and showed no evidence of lack of convergence or autocorrelation.

As with the statistical validation, the *ens5* model had improved performance over the constituent individual models in all IPCC AR6 reference regions (Figure 5A). Individual model skill varied greatly between regions, with some regions such as the North Pacific Ocean (NPO) and South Pacific Ocean (SPO) showing reduced predictive skills for all models, and the satellite monitoring CCI SST data, as well as greater hit rate variability (Figure 5B). DHW values during the baseline period showed similar distributions (mostly < 1°C-week) for the *ens5* hindcast and the CCI SST. In each case they were distinct from the distribution of DHW values during severe bleaching events, suggesting that both datasets enable the distinction of baseline from bleaching conditions (Figure 6).

3.3 | Data Records

Access to our dataset is through Figshare (https://doi.org/10.25909/25143128). The gridded datasets are available as NetCDF files.

The naming convention for the daily SST datasets is as follows:

`<model>_<scenario>_qdmCorrected_<timeperiod>.nc`

where *model* is the name of the CMIP6 model, or '*ens5*' for the 5-model ensemble; *scenario* is the name of the scenario (historical, SSP2-4.5, SSP3-7.0, SSP5-8.5); and *timeperiod* is the temporal span of the file (e.g., 1985–2014). The monthly summary files share the same naming convention with an additional qualifier that identifies whether the values are representative of the minimum, mean or maximum SST values seen within each month. All values are in °C.

The naming convention for the daily DHW is as follows:

`<model>_<scenario>_DHW_<timeperiod>.nc`

where *model* is the name of the CMIP6 model, or '*ens5*' for the 5-model ensemble; *scenario* is the name of the scenario (SSP2-4.5, SSP3-7.0, SSP5-8.5); and *timeperiod* is the temporal span of the file (e.g., 1985–2100). Note that due to the nature of the DHW calculation the SSP outputs are each appended to the historical period (1985–2014).

The naming convention for the summary DHW files is as follows:

`<model>_<scenario>_<timeperiod>_DHWSummary.nc`

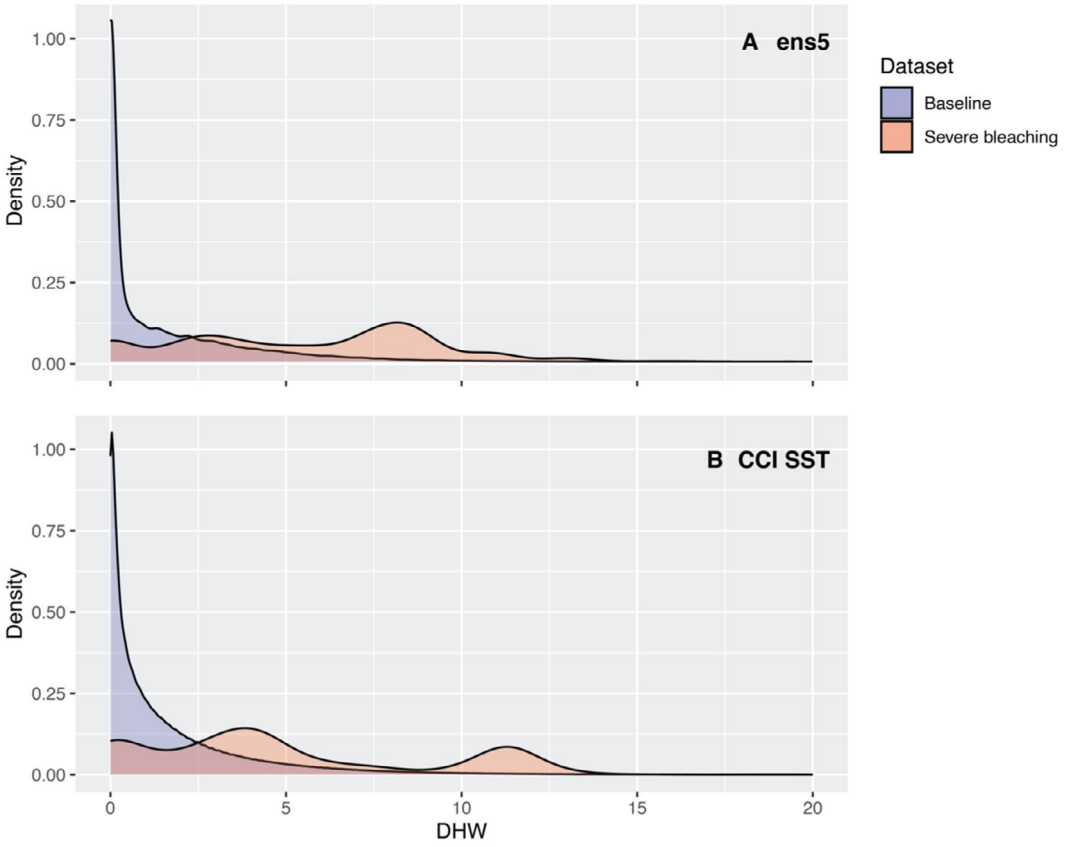

FIGURE 6 | Distribution of DHW during severe bleaching events and throughout the climatological baseline period. Density plots show DHW distributions only during severe bleaching events within 1985–2012 (red) and throughout the baseline period (i.e., all days considered between 1985 and 2012 at the same locations; blue) for (A) the *ens5* multi-model ensemble and (B) the CCI SST.

where *model* is the name of the CMIP6 model, or '*ens5*' for the 5-model ensemble; *scenario* is the name of the scenario (SSP2-4.5, SSP3-7.0, SSP5-8.5); and *timeperiod* is the temporal span of the file (e.g., 1985–2100). Note that due to the nature of the DHW calculation the SSP outputs are each appended to the historical period (1985–2014).

All gridded files have a 0.5° resolution with the following spatial dimensions—140 latitude (35° S to 35° N) × 720 longitude (180° E to 180° W). Time periods differ for each file type. Daily SST data has *n* days where *n* is either 10,927 for the historical period (1985–2014) or 31,325 for the future SSP periods (2015–2100). The monthly SST summary files have *n* months, where *n* is either 360 for the historical period (30 years) or 1032 for the future SSP periods (86 years). The annual summary DHW time dimension is 115 years (1986–2100).

4 | Concluding Remarks

CoralBleachRisk provides validated hindcasts and future projections of daily, monthly, and annual estimates of risk of bleaching for Earth's coral reefs. These include HotSpots (Liu et al. 2014) above the maximum monthly mean SST (i.e., the location-specific expected summertime maximum temperature) and resulting daily DHW between 1985 and 2100 for a total of > 74,500 0.5° grid-cells, containing ~1500 reef locations (Figure 1). It also provides access to downscaled and bias-corrected daily projections (1985–2100) of SST (in addition to monthly minima, maxima and means) from eight CMIP6 models. Annual summary metrics of coral bleaching risk derived from this daily data include minimum, maximum, mean and standard deviation of DHW, the onset and duration of DHW above the 4°C-week and 8°C-week thresholds. These metrics enable the identification of coral reef regions where future coral bleaching risk will increase at lesser rate than elsewhere (Mellin et al. 2024), a critical information to guide coral conservation and restoration efforts in the 21st century.

An accompanying online *CoralBleachRisk* data portal (https://coralbleachrisk.net/) allows users to graphically explore, download and analyse the timing, duration and extent of the coral bleaching risk for different years, scenarios and climate models (Figure 7). Data can be plotted and downloaded for a specific region (user-defined, IPCC reference regions [Iturbide et al. 2020] or Marine Ecoregions of the World [Spalding et al. 2007] [MEOW] provinces) or locations with individual reefs, using

FIGURE 7 | Snapshot of the *CoralBleachRisk* online data portal. Portal is available at https://coralbleachrisk.net/.

the data portal. Available metrics include annual summaries of coral bleaching risk, specifically minimum, maximum, mean, and standard deviation of DHW, the onset of DHW above the 4°C-week and the 8°C-week thresholds, and the duration of DHW above each threshold. Graphical assessments of the changes in annual maximum DHW, the annual onset of bleaching conditions, and the annual duration of bleaching conditions are also provided. A short tutorial is available in the data portal explaining how to crop, extract, and plot multiple metrics of SST and coral bleaching risk from different climate models.

CoralBleachRisk provides a data framework and supporting code that can be updated and built on. Future advances could include incorporating additional climate models, scenarios and realisations into *CoralBleachRisk* (Perkins-Kirkpatrick and Fischer 2013). However, this comes with the potential caveat that the number and combination of models for analysis might need to be reduced or changed. When *CoralBleachRisk* was developed, there were only sufficient CMIP6 climate model data to compare the first realisation of three SSP scenarios for a total of eight models. Moreover, only five of these models (used in the *ens5* projection) had suitable 'best' estimates of climate sensitivity (Hausfather et al. 2022). The size of this model ensemble projection is not problematic, because the performance of multi-model averaged climate projections tends to plateau with five or more models (Pierce et al. 2009). Likewise, our use of a single realisation in ensemble projections is unlikely to affect the accuracy of our projections because model performance increases to this asymptote faster with the addition of more models rather than more realisations (Pierce et al. 2009). Further methodological improvements could include refining the spatial resolution of *CoralBleachRisk* projections using dynamic downscaling (van Hooidonk et al. 2015). However, this could only be done regionally, because it is not yet computationally feasible at a global scale. As global temperatures continue to rise above maximum summertime averages, some level of coral adaptation is likely to occur over decadal time scales (Logan et al. 2014). Thus, the relevance of traditional methods for calculating DHW and associated bleaching thresholds might need to be re-evaluated. Accordingly, an assumption underlying the calculation of coral bleaching risk is that the threshold for coral bleaching reflects the maximum summer temperature from a historical baseline (1985–2012) (Liu et al. 2014). As more and better ecological data become available, future research should strive to determine the appropriate temporal scale over which a dynamic bleaching threshold (i.e., rolling MMM) can be calculated and implemented, capturing potential coral adaptation.

Author Contributions

Conceptualization: C.M., S.F.H., D.A.F. Methodology: C.M., S.B., S.F.H., D.A.F. Investigation: C.M., S.B., D.A.F. Visualisation: C.M., S.B. Funding acquisition: C.M., S.B., D.A.F.

Acknowledgments

Open access publishing facilitated by The University of Adelaide, as part of the Wiley - The University of Adelaide agreement via the Council of Australian University Librarians.

Conflicts of Interest

The authors declare no conflicts of interest.

Data Availability Statement

All data (available for Shared Socioeconomic Pathways SSP2-4.5, SSP3-7.0 and SSP5-8.5) and code for processing are available through Figshare (https://doi.org/10.25909/25143128) and via an online data portal (https://coralbleachrisk.net/).

References

Ainsworth, T. D., C. L. Hurd, R. D. Gates, and P. W. Boyd. 2020. "How Do We Overcome Abrupt Degradation of Marine Ecosystems and Meet the Challenge of Heat Waves and Climate Extremes?" *Global Change Biology* 26, no. 2: 343–354. https://doi.org/10.1111/gcb.14901.

Brown, B. E. 1997. "Coral Bleaching: Causes and Consequences." *Coral Reefs* 16, no. 1: S129–S138. https://doi.org/10.1007/s003380050249.

Brown, S. C., T. M. L. Wigley, B. L. Otto-Bliesner, and D. A. Fordham. 2020. "StableClim, Continuous Projections of Climate Stability From 21000 BP to 2100 CE at Multiple Spatial Scales." *Scientific Data* 7, no. 1: 335. https://doi.org/10.1038/s41597-020-00663-3.

Cannon, A. J., S. R. Sobie, and T. Q. Murdock. 2015. "Bias Correction of GCM Precipitation by Quantile Mapping: How Well Do Methods Preserve Changes in Quantiles and Extremes?" *Journal of Climate* 28, no. 17: 6938–6959. https://doi.org/10.1175/jcli-d-14-00754.1.

Darling, E. S., and I. M. Côté. 2018. "Seeking Resilience in Marine Ecosystems." *Science* 359, no. 6379: 986–987. https://doi.org/10.1126/science.aas9852.

Dixon, A. M., P. M. Forster, S. F. Heron, A. M. K. Stoner, and M. Beger. 2022. "Future Loss of Local-Scale Thermal Refugia in Coral Reef Ecosystems." *PLOS Climate* 1, no. 2: e0000004. https://doi.org/10.1371/journal.pclm.0000004.

Donner, S. D., G. J. M. Rickbeil, and S. F. Heron. 2017. "A New, High-Resolution Global Mass Coral Bleaching Database." *PLoS One* 12, no. 4: e0175490. https://doi.org/10.1371/journal.pone.0175490.

Donner, S. D., W. J. Skirving, C. M. Little, M. Oppenheimer, and O. Hoegh-Guldberg. 2005. "Global Assessment of Coral Bleaching and Required Rates of Adaptation Under Climate Change." *Global Change Biology* 11, no. 12: 2251–2265. https://doi.org/10.1111/j.1365-2486.2005.01073.x.

Eakin, C. M., J. A. Morgan, S. F. Heron, et al. 2010. "Caribbean Corals in Crisis: Record Thermal Stress, Bleaching, and Mortality in 2005." *PLoS One* 5, no. 11: e13969. https://doi.org/10.1371/journal.pone.0013969.

Eyring, V., S. Bony, G. A. Meehl, et al. 2016. "Overview of the Coupled Model Intercomparison Project Phase 6 (CMIP6) Experimental Design and Organization." *Geoscientific Model Development* 9, no. 5: 1937–1958. https://doi.org/10.5194/gmd-9-1937-2016.

Ferrari, S., and F. Cribari-Neto. 2004. "Beta Regression for Modelling Rates and Proportions." *Journal of Applied Statistics* 31, no. 7: 799–815. https://doi.org/10.1080/0266476042000214501.

Fordham, D. A., F. Saltré, S. Haythorne, et al. 2017. "PaleoView: A Tool for Generating Continuous Climate Projections Spanning the Last 21 000 Years at Regional and Global Scales." *Ecography* 40, no. 11: 1348–1358. https://doi.org/10.1111/ecog.03031.

Fordham, D. A., T. M. Wigley, and B. W. Brook. 2011. "Multi-Model Climate Projections for Biodiversity Risk Assessments." *Ecological Applications* 21, no. 8: 3317–3331.

Fordham, D. A., T. M. Wigley, M. J. Watts, and B. W. Brook. 2012. "Strengthening Forecasts of Climate Change Impacts With Multi-Model Ensemble Averaged Projections Using MAGICC/SCENGEN 5.3." *Ecography* 35, no. 1: 4–8.

Good, S. A., O. Embury, C. E. Bulgin, and J. Mittaz. 2019. "ESA Sea Surface Temperature Climate Change Initiative (SST_cci): Level 4 Analysis Climate Data Record, Version 2.1." Centre for Environmental

Data Analysis. https://doi.org/10.5285/62c0f97b1eac4e0197a674870afe1ee6.

Goodrich, B., J. Gabry, I. Ali, and S. Brilleman. 2023. "rstanarm: Bayesian Applied Regression Modeling via Stan. (Version R Package Version 2.21.4)." https://mc-stan.org/rstanarm.

Gupta, H. V., H. Kling, K. K. Yilmaz, and G. F. Martinez. 2009. "Decomposition of the Mean Squared Error and NSE Performance Criteria: Implications for Improving Hydrological Modelling." *Journal of Hydrology* 377, no. 1: 80–91. https://doi.org/10.1016/j.jhydrol.2009.08.003.

Hausfather, Z., K. Marvel, G. A. Schmidt, J. W. Nielsen-Gammon, and M. Zelinka. 2022. "Climate Simulations: Recognize the 'Hot Model' Problem." *Nature* 605, no. 7908: 26–29. https://doi.org/10.1038/d41586-022-01192-2.

Heron, S. F., L. Johnston, G. Liu, et al. 2016. "Validation of Reef-Scale Thermal Stress Satellite Products for Coral Bleaching Monitoring." *Remote Sensing* 8, no. 1: 59.

Heron, S. F., G. Liu, C. M. Eakin, et al. 2015. "Climatology Development for NOAA Coral Reef Watch's 5-km Product Suite." https://doi.org/10.7289/V59C6VBS.

Heron, S. F., G. Liu, J. L. Rauenzahn, et al. 2014. "Improvements to and Continuity of Operational Global Thermal Stress Monitoring for Coral Bleaching." *Journal of Operational Oceanography* 7, no. 2: 3–11. https://doi.org/10.1080/1755876X.2014.11020154.

Heron, S. F., J. A. Maynard, R. van Hooidonk, and C. M. Eakin. 2016. "Warming Trends and Bleaching Stress of the World's Coral Reefs 1985–2012." *Scientific Reports* 6, no. 1: 38402. https://doi.org/10.1038/srep38402.

Hijmans, R. 2022. "terra: Spatial Data Analysis. R Package 1.6-48." https://rspatial.org/terra/.

Hoegh-Guldberg, O., E. V. Kennedy, H. L. Beyer, C. McClennen, and H. P. Possingham. 2018. "Securing a Long-Term Future for Coral Reefs." *Trends in Ecology & Evolution* 33, no. 12: 936–944. https://doi.org/10.1016/j.tree.2018.09.006.

Hoegh-Guldberg, O., W. Skirving, S. G. Dove, et al. 2023. "Coral Reefs in Peril in a Record-Breaking Year." *Science* 382: 1238–1240. https://doi.org/10.1126/science.adk4532.

Hughes, T. P., K. D. Anderson, S. R. Connolly, et al. 2018. "Spatial and Temporal Patterns of Mass Bleaching of Corals in the Anthropocene." *Science* 359, no. 6371: 80–83. https://doi.org/10.1126/science.aan8048.

Hughes, T. P., M. L. Barnes, D. R. Bellwood, et al. 2017. "Coral Reefs in the Anthropocene." *Nature* 546: 82–90. https://doi.org/10.1038/nature22901.

Hughes, T. P., J. T. Kerry, S. R. Connolly, et al. 2021. "Emergent Properties in the Responses of Tropical Corals to Recurrent Climate Extremes." *Current Biology* 31, no. 23: 5393–5399.e5393. https://doi.org/10.1016/j.cub.2021.10.046.

Hughes, T. P., J. T. Kerry, S. R. Connolly, et al. 2018. "Ecological Memory Modifies the Cumulative Impact of Recurrent Climate Extremes." *Nature Climate Change* 9: 40–43. https://doi.org/10.1038/s41558-018-0351-2.

Iturbide, M., J. Bedia, S. Herrera, et al. 2019. "The R-Based climate4R Open Framework for Reproducible Climate Data Access and Post-Processing." *Environmental Modelling & Software* 111: 42–54. https://doi.org/10.1016/j.envsoft.2018.09.009.

Iturbide, M., J. M. Gutiérrez, L. M. Alves, et al. 2020. "An Update of IPCC Climate Reference Regions for Subcontinental Analysis of Climate Model Data: Definition and Aggregated Datasets." *Earth System Science Data* 12, no. 4: 2959–2970. https://doi.org/10.5194/essd-12-2959-2020.

Jones, P. W. 1999. "First- and Second-Order Conservative Remapping Schemes for Grids in Spherical Coordinates." *Monthly Weather Review* 127, no. 9: 2204–2210. https://doi.org/10.1175/1520-0493(1999)127<2204:Fasocr>2.0.Co;2.

Lachs, L., J. C. Bythell, H. K. East, et al. 2021. "Fine-Tuning Heat Stress Algorithms to Optimise Global Predictions of Mass Coral Bleaching." *Remote Sensing* 13, no. 14: 2677.

Leggat, W. P., E. F. Camp, D. J. Suggett, et al. 2019. "Rapid Coral Decay Is Associated With Marine Heatwave Mortality Events on Reefs." *Current Biology* 29, no. 16: 2723–2730.e2724. https://doi.org/10.1016/j.cub.2019.06.077.

Lemon, J. 2006. "Plotrix: A Package in the Red Light District of R." *R-News* 6: 8–12.

Little, C. M., G. Liu, J. L. De La Cour, C. M. Eakin, D. Manzello, and S. F. Heron. 2022. "Global Coral Bleaching Event Detection From Satellite Monitoring of Extreme Heat Stress." *Frontiers in Marine Science* 9: 883271. https://doi.org/10.3389/fmars.2022.883271.

Liu, G., C. M. Eakin, M. Chen, et al. 2018. "Predicting Heat Stress to Inform Reef Management: NOAA Coral Reef Watch's 4-Month Coral Bleaching Outlook." *Frontiers in Marine Science* 5: 57. https://doi.org/10.3389/fmars.2018.00057.

Liu, G., S. Heron, C. M. Eakin, et al. 2014. "Reef-Scale Thermal Stress Monitoring of Coral Ecosystems: New 5-Km Global Products From NOAA Coral Reef Watch." *Remote Sensing* 6: 11579–11606. https://doi.org/10.3390/rs61111579.

Logan, C. A., J. P. Dunne, C. M. Eakin, and S. D. Donner. 2014. "Incorporating Adaptive Responses Into Future Projections of Coral Bleaching." *Global Change Biology* 20, no. 1: 125–139. https://doi.org/10.1111/gcb.12390.

Mellin, C., S. Brown, N. Cantin, et al. 2024. "Cumulative Risk of Future Bleaching for the World's Coral Reefs." *Science Advances* 10, no. 26: eadn9660. https://doi.org/10.1126/sciadv.adn9660.

Merchant, C. J., O. Embury, C. E. Bulgin, et al. 2019. "Satellite-Based Time-Series of Sea-Surface Temperature Since 1981 for Climate Applications." *Scientific Data* 6, no. 1: 223. https://doi.org/10.1038/s41597-019-0236-x.

O'Neill, B. C., E. Kriegler, K. L. Ebi, et al. 2017. "The Roads Ahead: Narratives for Shared Socioeconomic Pathways Describing World Futures in the 21st Century." *Global Environmental Change* 42: 169–180. https://doi.org/10.1016/j.gloenvcha.2015.01.004.

Pebesma, E. 2018. "Simple Features for R: Standardized Support for Spatial Vector Data." *R Journal* 1: 439–446. https://doi.org/10.32614/RJ-2018-009.

Perkins-Kirkpatrick, S., and E. Fischer. 2013. "The Usefulness of Different Realizations for the Model Evaluation of Regional Trends in Heat Waves." *Geophysical Research Letters* 40: 5793–5797. https://doi.org/10.1002/2013GL057833.

Pielke, R., Jr., M. G. Burgess, and J. Ritchie. 2022. "Plausible 2005–2050 Emissions Scenarios Project Between 2°C and 3°C of Warming by 2100." *Environmental Research Letters* 17, no. 2: 024027. https://doi.org/10.1088/1748-9326/ac4ebf.

Pierce, D. W., T. P. Barnett, B. D. Santer, and P. J. Gleckler. 2009. "Selecting Global Climate Models for Regional Climate Change Studies." *Proceedings of the National Academy of Sciences* 106, no. 21: 8441–8446. https://doi.org/10.1073/pnas.0900094106.

R Development Core Team. 2022. *R: A Language and Environment for Statistical Computing*. Vienna, Austria: R Foundation for Statistical Computing. http://www.R-project.org/.

Rayner, N., Y. Tsushima, C. Atkinson, et al. 2019. "Sea Surface Temperature CCI Phase-II Climate Assessment Report." SST_CCI-CAR-UKMO-201 (CAR). http://www.esa-sst-cci.org.

Riahi, K., D. P. van Vuuren, E. Kriegler, et al. 2017. "The Shared Socioeconomic Pathways and Their Energy, Land Use, and Greenhouse Gas Emissions Implications: An Overview." *Global Environmental Change* 42: 153–168. https://doi.org/10.1016/j.gloenvcha.2016.05.009.

Rodriguez, O., D. Jimenez, and J. Quiros. 2024. "loadeR: Load Data for Analysis System. R Pagkage Version 1.1.8." https://CRAN.R-project.org/package=loadeR.

Santer, B. D., J. F. Painter, C. A. Mears, et al. 2013. "Identifying Human Influences on Atmospheric Temperature." *Proceedings of the National Academy of Sciences* 110, no. 1: 26–33. https://doi.org/10.1073/pnas.1210514109.

Schulzweida, U. 2021. "Climate Data Operators (Version 1.9.10)." https://code.mpimet.mpg.de/projects/cdo.

Skirving, W., B. Marsh, J. De La Cour, et al. 2020. "CoralTemp and the Coral Reef Watch Coral Bleaching Heat Stress Product Suite Version 3.1." *Remote Sensing* 12, no. 23: 3856.

South, A. 2017. "rnaturalearth: World Map Data From Natural Earth. R Package Version 0.1.0." https://CRAN.R-project.org/package=rnaturalearth.

Spalding, M. D., and B. E. Brown. 2015. "Warm-Water Coral Reefs and Climate Change." *Science* 350, no. 6262: 769–771. https://doi.org/10.1126/science.aad0349.

Spalding, M. D., H. E. Fox, G. R. Allen, et al. 2007. "Marine Ecoregions of the World: A Bioregionalization of Coastal and Shelf Areas." *Bioscience* 57, no. 7: 573–583. https://doi.org/10.1641/B570707.

Spillman, C. M., and G. A. Smith. 2021. "A New Operational Seasonal Thermal Stress Prediction Tool for Coral Reefs Around Australia." *Frontiers in Marine Science* 8: 687833. https://doi.org/10.3389/fmars.2021.687833.

Suggett, D. J., and D. J. Smith. 2011. "Interpreting the Sign of Coral Bleaching as Friend vs. Foe." *Global Change Biology* 17, no. 1: 45–55. https://doi.org/10.1111/j.1365-2486.2009.02155.x.

van Hooidonk, R., J. Maynard, J. Tamelander, et al. 2016. "Local-Scale Projections of Coral Reef Futures and Implications of the Paris Agreement." *Scientific Reports* 6: 39666. https://doi.org/10.1038/srep39666.

van Hooidonk, R., J. A. Maynard, Y. Liu, and S.-K. Lee. 2015. "Downscaled Projections of Caribbean Coral Bleaching That Can Inform Conservation Planning." *Global Change Biology* 21, no. 9: 3389–3401. https://doi.org/10.1111/gcb.12901.

van Hooidonk, R., J. A. Maynard, D. Manzello, and S. Planes. 2014. "Opposite Latitudinal Gradients in Projected Ocean Acidification and Bleaching Impacts on Coral Reefs." *Global Change Biology* 20, no. 1: 103–112. https://doi.org/10.1111/gcb.12394.

van Hooidonk, R., J. A. Maynard, and S. Planes. 2013. "Temporary Refugia for Coral Reefs in a Warming World." *Nature Climate Change* 3, no. 5: 508–511. https://doi.org/10.1038/Nclimate1829.

van Vuuren, D. P., J. Edmonds, M. Kainuma, et al. 2011. "The Representative Concentration Pathways: An Overview." *Climatic Change* 109, no. 1: 5–31. https://doi.org/10.1007/s10584-011-0148-z.

Wilcox, R. R. 1994. "The Percentage Bend Correlation Coefficient." *Psychometrika* 59, no. 4: 601–616. https://doi.org/10.1007/BF02294395.

Willmott, C. J. 2013. "On the Validation of Models." *Physical Geography* 2, no. 2: 184–194. https://doi.org/10.1080/02723646.1981.10642213.

Zender, C., H. Butowsky, and P. Vincente. 2021. "netCDF Operators (Version 4.9.1 'Skyglow')." https://nco.sourceforge.net/.